18 Renal Lymphoma

Sheila Sheth and Elliot K. Fishman

CONTENTS

18.1 Introduction

Malignant lymphomas, broadly categorized into Hodgkin and non-Hodgkin lymphomas, constitute a heterogeneous group of cancers arising from the lymphoreticular system. The incidence of these tumors has been growing (approximately 50,000 new cases are diagnosed in the United States each year) and effective treatments prolong the survival of many affected patients. Thus, imaging studies are routinely requested for diagnosis and management. While the most common manifestation of malignant lymphomas is lymphadenopathy, visceral involvement is diagnosed with increasing frequency. Excluding the hematopoietic and reticuloendothelial organs, the genitourinary tract is the most commonly affected system (Richmond et al. 1962).

S. Sheth, MD
Associate Professor of Radiology and Pathology, Johns Hopkins University School of Medicine, Director, Biopsy Service, Department of Radiology, Johns Hopkins Hospital, 600 North Wolfe Street, HAL B176D, Baltimore, MD 21287, USA
E. K. Fishman, MD, FACR
Professor of Radiology and Oncology, Johns Hopkins University School of Medicine, Director, Diagnostic Radiology and Body CT, Department of Radiology, Johns Hopkins Outpatient Center, 601 North Caroline Street, Room 3254, Baltimore, MD 21287, USA

18.2 Secondary vs Primary Renal Lymphoma

Renal lymphoma usually occurs in the setting of widespread non-Hodgkin lymphoma (NHL), typically B-cell type intermediate or high-grade tumors or Burkitt lymphoma (Figs. 18.1, 18.2). Involvement with Hodgkin disease is much less common, found in less than 1% of patients at presentation (Chepuri et al. 2003; Guermazi et al. 2001).

Fig. 18.1. Widespread B-cell non-Hodgkin lymphoma in a 65-year-old woman. Axial contrast-enhanced CT scan of the mid-abdomen shows soft tissue masses in both kidneys (*black arrows*). The tumor infiltrates around the left renal pelvis without causing obstruction. Note the retroperitoneal adenopathy (*arrowhead*) as well as the large mass in the abdominal wall (*white arrow*).

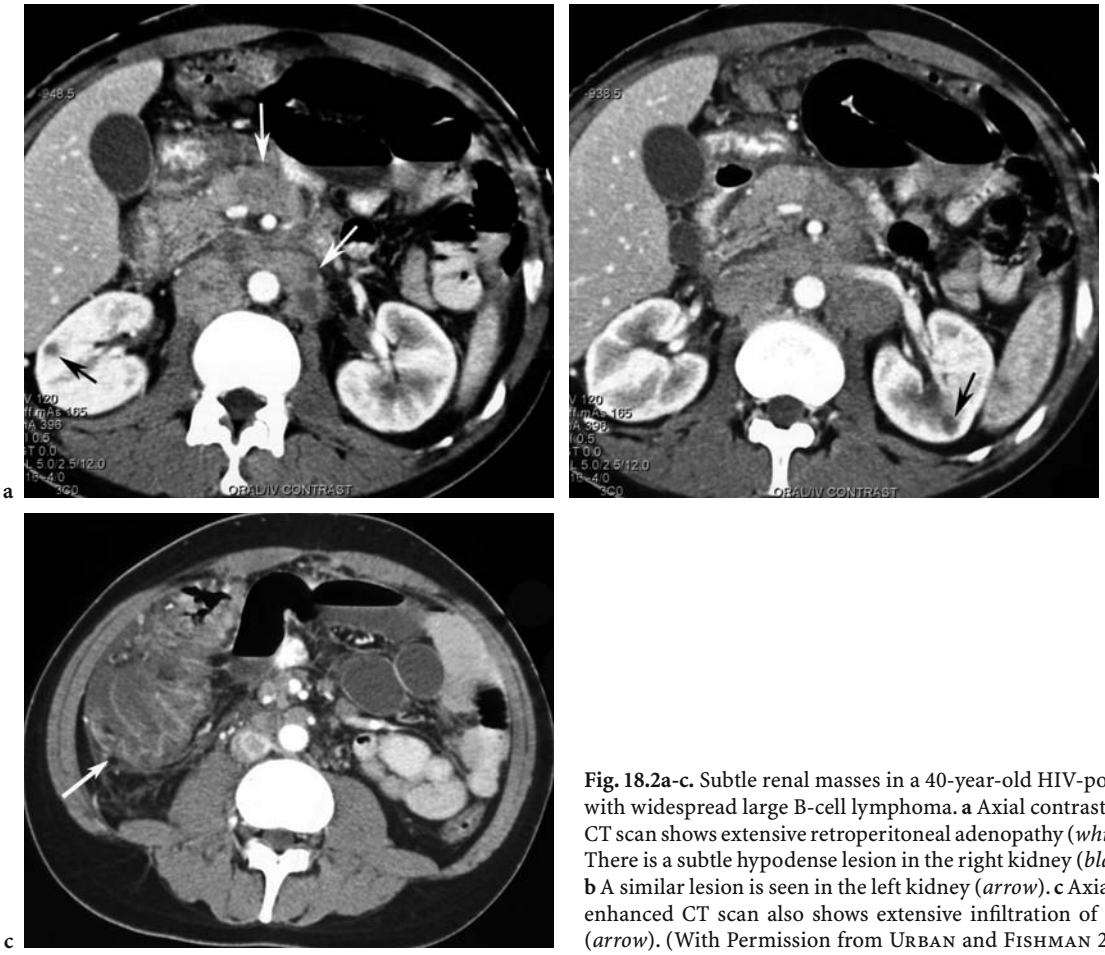

Fig. 18.2a-c. Subtle renal masses in a 40-year-old HIV-positive man with widespread large B-cell lymphoma. **a** Axial contrast-enhanced CT scan shows extensive retroperitoneal adenopathy (*white arrows*). There is a subtle hypodense lesion in the right kidney (*black arrow*). **b** A similar lesion is seen in the left kidney (*arrow*). **c** Axial contrast-enhanced CT scan also shows extensive infiltration of the cecum (*arrow*). (With Permission from Urban and Fishman 2000)

Foci of lymphoma are found in the kidneys of 37 to nearly 50% of patients in autopsy series (Richmond et al. 1962; Eisenberg et al. 1994). Surprisingly, the diagnosis of renal lymphoma by cross-sectional imaging has been reported to reach only 3–8% of cases (Chepuri et al. 2003; Cohan et al. 1990; Reznek et al. 1990; Urban and Fishman 2000). This apparent discrepancy between the pathological and radiological literature can be explained by several factors: renal lymphoma is often poorly documented as renal biopsy or nephrectomy are rarely indicated to confirm the diagnosis in the context of systemic disease; these numbers were gathered before the widespread use of helical single and multidetector computed tomography (CT) when older-generation scanners underestimated the frequency of renal lesions. It is anticipated that superior evaluation of the renal parenchyma afforded by modern imaging techniques will allow detection of renal lymphoma in many more patients (Urban and Fishman 2000).

In the majority of cases, renal lymphoma is clinically asymptomatic. Its detection on imaging studies may, however, influence staging and type and length of treatment. Follow-up data in patients with renal lymphoma suggest that while involvement of the kidneys at the time of presentation does not necessarily indicate a poor prognosis, renal recurrence is associated with increased mortality (Chepuri et al. 2003; Richards et al. 1990).

Primary renal lymphoma, arising in the renal parenchyma and not associated with systemic manifestation, is uncommon, accounting for less than 1% of cases of extranodal disease. Its origin is somewhat speculative. As the renal parenchyma normally does not contain lymphoid tissue, several mechanisms have been postulated to account for the development of lymphoma in the kidney: the tumor may originate in the lymphatic-rich renal capsule or the perinephric fat and invade the parenchyma, or can arise from lymphocytes present in areas of chronic inflammation (Stallone et al. 2000). It is

usually a B-cell NHL and affects middle-age to older patients. Patients present with flank pain, hematuria, or non-specific symptoms of fever and night sweats (Yasunaga et al. 1997). Renal insufficiency from extensive lymphomatous infiltration of both kidneys is rare (Malbrain et al. 1994; Mills et al. 1992). The prognosis is generally poor.

18.3 Imaging Techniques for Renal Lymphoma

Several radiographic techniques are available to evaluate the kidneys. Cross-sectional imaging modalities, such as CT, ultrasound (US), or magnetic resonance (MR) imaging, are progressively replacing the traditional intravenous urography, although the latter remains the most sensitive method for detecting subtle lesions of the collecting system and diagnosing delay in renal excretion caused by hydronephrosis.

18.3.1 Computed Tomography

Helical (single or multidetector) CT is the imaging modality of choice in evaluating patients with suspected or known renal lymphoma. It not only depicts the renal lesions but also most accurately identifies extension to adjacent anatomic structures such as the perirenal space and the retroperitoneum and defines the systemic spread of the disease. Administration of intravenous contrast is essential to allow the depiction of subtle renal parenchymal abnormalities. Image acquisition in the corticomedullary and nephrographic phases of renal enhancement is generally sufficient. Small masses and subtle infiltration can be missed without the nephrographic phase, whereas the corticomedullary phase allows optimal demonstration of vascular encasement. If the tumor is predominantly central and affects the hilar region, or when the collecting system appears to be involved, excretory phase acquisition is necessary. This latter phase also best demonstrates obstruction of the collecting system by retroperitoneal masses. Images obtained prior to contrast injection are seldom required but may better demonstrate calcifications or areas of recent hemorrhage. In patients who are unable to receive intravenous contrast material, renal lymphoma can often be suspected in the presence of asymmetric size of the kidneys, focal bulge, and large retroperitoneal adenopathy.

18.3.2 Ultrasound

Ultrasound is less sensitive than CT both in detecting the presence of disease as well as the number of lesions (Heiken et al. 1983; Weinberger et al. 1990); however, it may be the first test requested for the rare patient who presents with renal insufficiency. Ultrasound is also helpful in patients who are unable to receive intravenous iodinated contrast and is the ideal guidance modality during percutaneous biopsy.

18.3.3 Magnetic Resonance Imaging

The role of MR imaging in renal lymphoma is not clearly established. It may be useful in patients with iodinated contrast allergy or renal insufficiency. In addition, MR imaging has been proven superior to CT in depicting involvement of the bone marrow.

18.3.4 Positron Emission Tomography

Positron emission tomography (PET) is a very useful technique for staging of lymphomas and detection of recurrences. Because it detects increased metabolic activity within lymphomatous deposits, fluorodeoxyglucose PET is more sensitive and specific than conventional anatomic imaging studies in detecting small additional tumor deposits (Moog et al. 1998). The combination of PET and CT data acquisition at the same time (PET/CT) is emerging as a powerful tool for observing the metabolic activity of tumors with anatomic detail, allowing precise location and potentially earlier detection (Fig. 18.3; Metser et al. 2004).

18.4 Imaging Characteristics of Renal Lymphoma

18.4.1 Radiologic–Pathologic Correlation

Renal lymphomas display a variety of imaging appearances depending on their histological pattern of proliferation (Hartman et al. 1982).

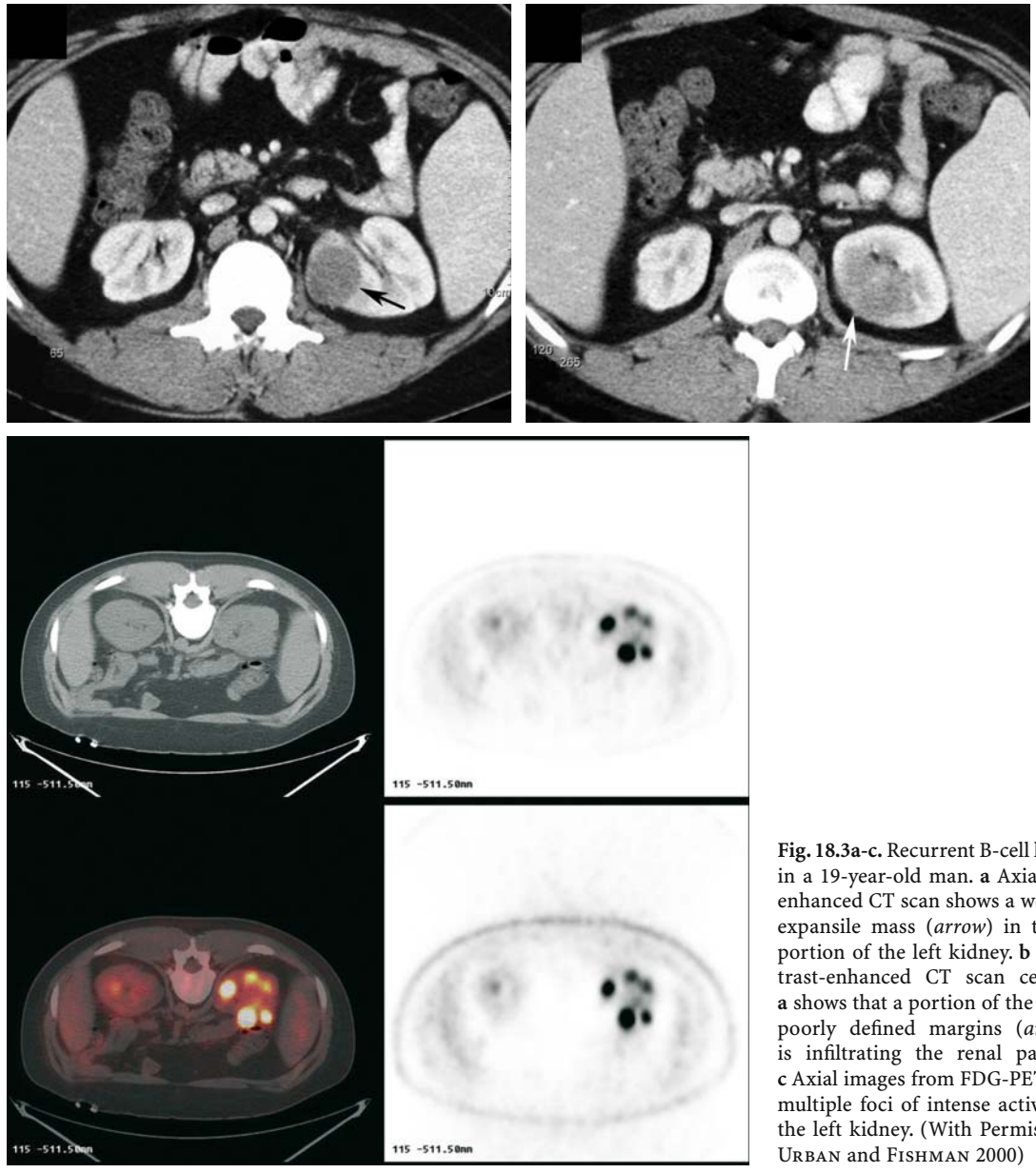

Fig. 18.3a-c. Recurrent B-cell lymphoma in a 19-year-old man. **a** Axial contrast-enhanced CT scan shows a well-defined expansile mass (*arrow*) in the medial portion of the left kidney. **b** Axial contrast-enhanced CT scan cephalad to **a** shows that a portion of the tumor has poorly defined margins (*arrow*) and is infiltrating the renal parenchyma. **c** Axial images from FDG-PET/CT show multiple foci of intense activity within the left kidney. (With Permission from Urban and Fishman 2000)

Malignant lymphocytes reach the renal parenchyma via hematogenous spread and proliferate within the interstitium, using the nephrons, collecting tubules, and blood vessels as a scaffolding for further growth. Alternatively, some tumors spread by contiguous extension from the retroperitoneum penetrating through the renal capsule. Once the tumor reaches the kidneys, its radiological appearance is determined by its predominant proliferation mechanism. If the tumor follows an infiltrative growth pattern, and malignant cells proliferate along the scaffolding of the normal interstitial tissue, the kidneys enlarge but their reniform shape is preserved. The lesions have ill-defined borders and may be quite subtle (Pickhardt et al. 2000). In many cases, however, malignant lymphocytes proliferate focally, destroying the adjacent renal parenchyma and forming single, or more commonly, bilateral expansile lesions with well-defined margins. Small masses may coalesce, grow, and distort the renal contour (Hartman et al. 1982). In practice. a combination of the two types is not unusual.

Most cases of renal lymphoma occur in patients with systemic disease and do not generally pose a diagnostic dilemma (Sheeran and Sussman 1998). If, however, renal involvement is isolated or the appearance of the

renal lesions is atypical, further investigations, including percutaneous biopsy, may be indicated.

Radiological appearances associated with renal lymphoma include multiple masses, solitary lesion, direct extension from retroperitoneal adenopathy, predominant involvement of the perinephric space, and diffuse infiltration of one or both kidneys. Lymphoma less commonly affects the renal sinus and collecting system. In a large autopsy series of 696 patients with lymphoma, Richmond et al. (1962) observed multiple renal masses in 61% of cases. Solitary renal nodule or mass or direct invasion from retroperitoneal adenopathy were equally common.

Fig. 18.4. The characteristic appearance of multiple masses in renal lymphoma. (With permission from Urban and Fishman 2000)

18.4.2 Multiple Renal Masses

The most common appearance of renal lymphoma on imaging is multiple masses of variable size, typically 1–3 cm in diameter (Fig. 18.4). This pattern is seen in 50–60% of cases. The lesions are most often bilateral but can be unilateral (Chepuri et al. 2003; Cohan et al. 1990; Heiken et al. 1983; Reznek et al. 1990; Urban and Fishman 2000).

On unenhanced CT, these masses appear as soft tissue lesions slightly more hyperdense than the surrounding parenchyma. Calcifications are rare. Administration of intravenous contrast is essential for detection if the lesions are small and do not distort the renal outline (Fig. 18.5). Small tumors are best demonstrated in the nephrographic phase of renal enhancement (Szolar et al. 1997). Lymphomatous deposits enhance less than the normal renal tissue and appear as relatively homogeneous masses that are hypodense compared with the surrounding cortex (Figs. 18.1, 18.5, 18.6). Large lesions tend to be more heterogeneous and may contain hypodense areas suggesting necrosis, particularly after chemotherapy. The presence of retroperitoneal adenopathy is an additional clue to the diagnosis.

Few reports have described the MR imaging appearance of renal lymphomas (Semelka et al. 1996). Tumors are hypointense compared with normal cortex on T1-weighted images and iso- or hypointense on T2-weighted images. They enhance less than the renal parenchyma following gadolinium administration.

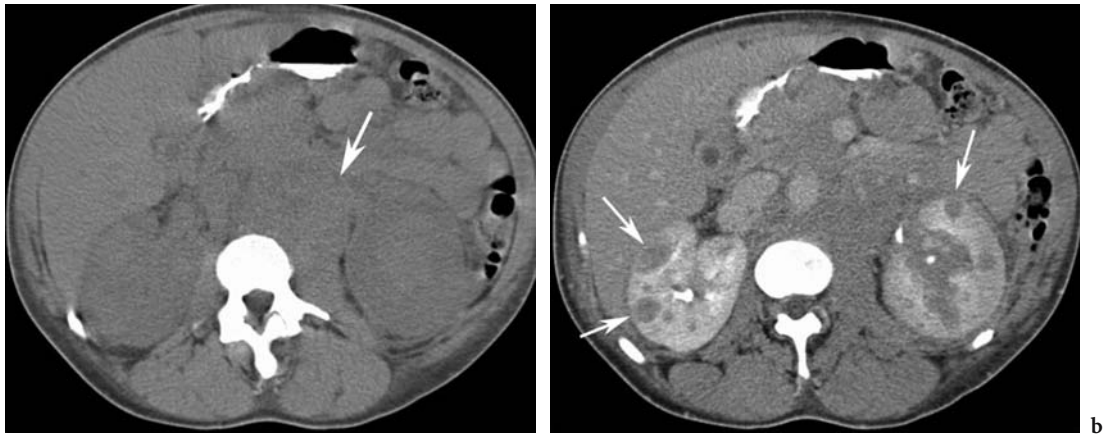

a **b**

Fig. 18.5a,b. Large B-cell non-Hodgkin lymphoma in a 41-year-old HIV-positive man. **a** Axial unenhanced CT scan of the mid-abdomen shows a soft mass in the region of the great vessels suspicious for retroperitoneal adenopathy (*arrow*). The kidneys do not demonstrate any abnormality in contour. **b** Axial contrast-enhanced CT scan of the mid-abdomen shows bilateral soft tissue masses in both kidneys (*arrows*). Note that these masses do not deform the contour of the kidneys. The para-aortic retroperitoneal adenopathy is seen much better. (With Permission from Urban and Fishman 2000)

Fig. 18.6. Renal non-Hodgkin lymphoma in a 46-year-old woman. Axial contrast-enhanced CT scan of the kidneys shows multiple soft tissue masses in both kidneys (*arrows*).

On US, lymphomatous masses are typically hypoechoic and homogeneous (Fig. 18.7). The US appearance reflects the underlying homogeneity of lymphoma deposits which offer very few tissue interfaces to the insonating beam. Color or power Doppler US shows displacement of normal renal vessels with little vascularity within the lesions.

Radiologically, multifocal renal lymphoma must be differentiated from metastatic disease to the kidneys. Primary tumors that frequently spread to the kidneys include lung and breast cancer as well as melanoma (Fig. 18.8). In the absence of relevant clinical history, image-guided biopsy is indicated. Unlike lymphoma, multiple synchronous renal cell carcinomas are generally hypervascular (Fig. 18.9).

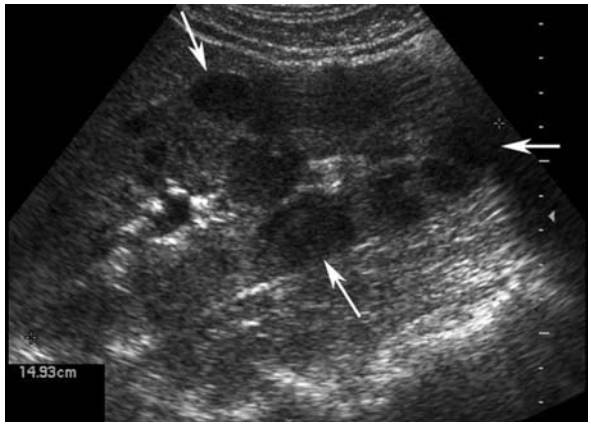

a

b

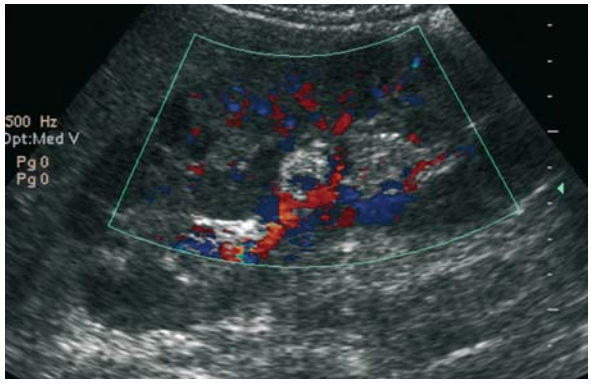

c

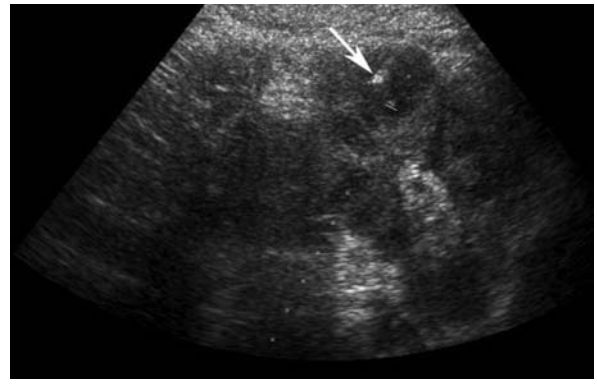

d

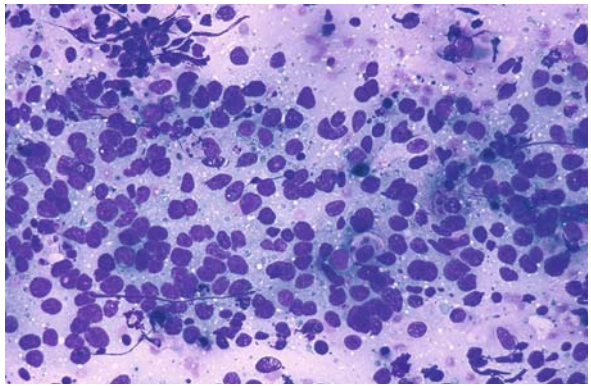

e

Fig. 18.7a-e. Renal non-Hodgkin lymphoma in a 33-year-old man. **a** Sagittal and **b** transverse ultrasound images of the right kidney show multiple hypoechoic soft tissue masses in the parenchyma (*arrows*). Note that the kidney is enlarged but preserves its reniform shape. **c** The color Doppler US image shows displacement of the renal vessels by the masses. **d** Transverse ultrasound image of the right kidney during the ultrasound-guided biopsy procedure shows that the echogenic needle tip (*arrow*) is clearly seen within the hypoechoic mass. **e** Analysis of the fine-needle-aspiration sample shows malignant lymphocytes (Diff-Quik stain on site). (With Permission from Urban and Fishman 2000)

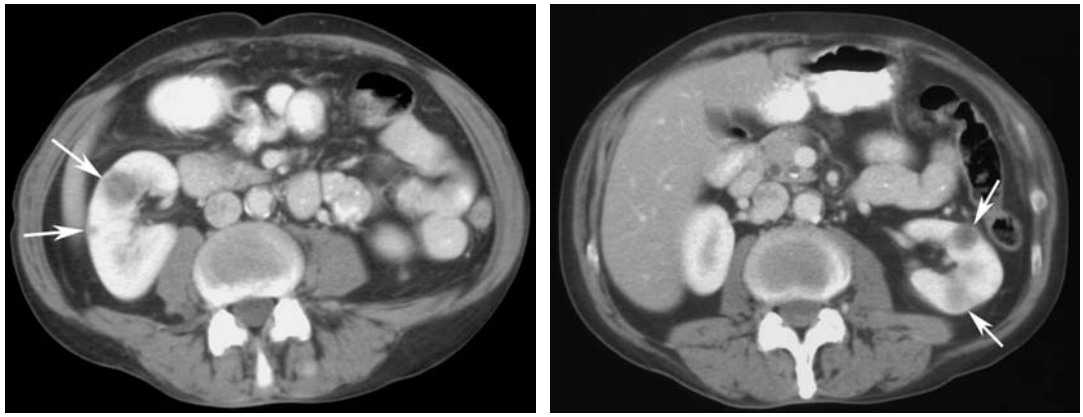

Fig. 18.8a,b. Metastatic melanoma in a 65-year-old man. **a** Axial contrast-enhanced CT scan at the nephrographic phase shows at least two soft tissue masses in the right kidney (*arrows*). **b** Axial contrast-enhanced CT scan in the nephrographic phase shows similar findings in the left kidney (*arrows*).

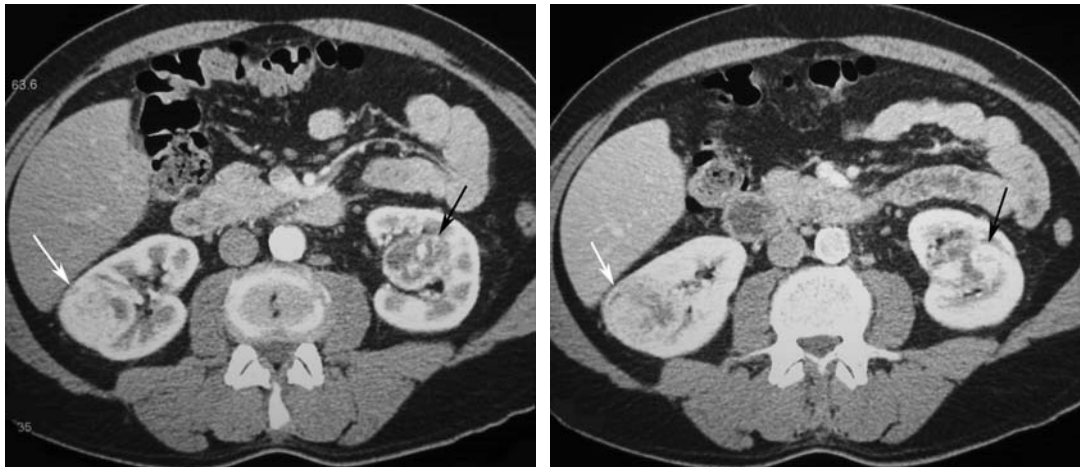

Fig. 18.9a,b. Multifocal renal cell carcinoma in a 68-year-old man with right upper quadrant pain. Axial CT scan of the kidneys at the **a** arterial phase and **b** venous enhancement show bilateral hypervascular heterogeneous masses (*arrows*). This enhancement pattern is seen more commonly in renal cell carcinoma. The diagnosis was confirmed on percutaneous ultrasound-guided biopsy and the patient was treated with partial right nephrectomy and total left nephrectomy. (With Permission from Urban and Fishman 2000)

18.4.3 Solitary Mass

A solitary renal mass is reported in 10–20% of patients with renal lymphoma (Fig. 18.10). The mass characteristically demonstrates little enhancement following intravenous contrast administration (Figs. 18.11, 18.12). This feature is helpful in differentiating lymphoma from conventional renal cell carcinoma which usually enhances in the arterial phase (Fig. 18.13); however, some primary renal tumors, such as the papillary variant of renal cell carcinoma, may not exhibit this classic enhancement (Fig. 18.14). Percutaneous biopsy is required for definitive diagnosis to exclude an atypical renal cell carcinoma or a solitary metastasis.

18.4.4 Cystic Mass

Cystic appearance is distinctly unusual in renal lymphoma: Of 28 cystic Bosniak III lesions reviewed by Harsinghani et al. (2003), only one turned out to be a lymphoma at biopsy; however, focal lesions can appear markedly hypoechoic on US and even exhibit some degree of enhancement through transmission mimicking a cystic mass.

Fig. 18.10. The characteristic appearance of a dominant solitary lymphomatous renal mass. (With Permission from Urban and Fishman 2000)

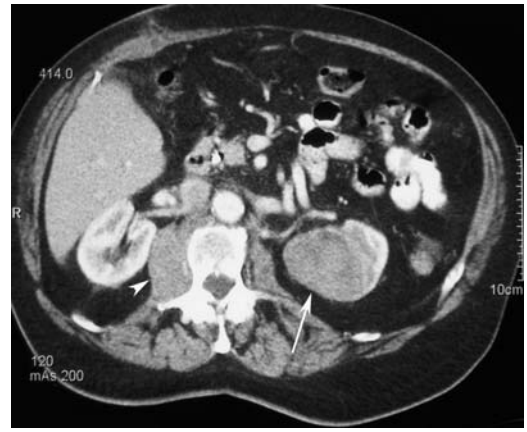

Fig. 18.11. Carlson large B-cell non-Hodgkin lymphoma in a 72-year-old man with a history of prostate cancer. Axial contrast-enhanced CT scan of the kidneys shows an expansile well-defined mass (*arrow*) in the left kidney. No other renal solid masses were present, but the right psoas muscle is enlarged (*arrowhead*). The diagnosis was established by ultrasound-guided percutaneous biopsy of the left renal mass. (With Permission from Urban and Fishman 2000)

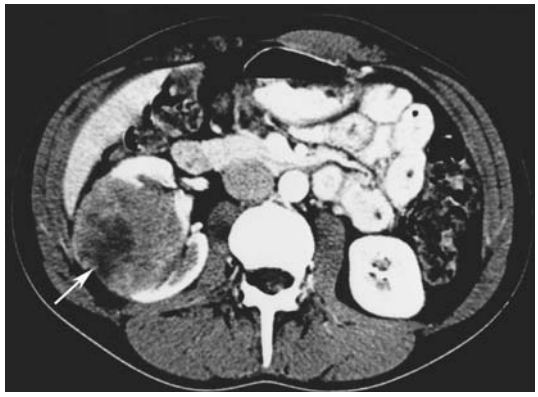

Fig. 18.12. Recurrent non-Hodgkin lymphoma in the right kidney mimicking a renal cell carcinoma in 41-year-old woman with a history of lymphoma. Axial contrast-enhanced CT scan of the kidneys shows a solitary heterogeneous mass (*arrow*) in the right kidney. The diagnosis was established by percutaneous biopsy.

Fig. 18.13. Renal cell carcinoma in an 80-year-old man. Axial contrast-enhanced CT scan in the corticomedullary phase shows a single hypervascular mass (*arrow*) in the right kidney. This is the classic appearance of renal cell carcinoma and nephrectomy was recommended. (With Permission from Urban and Fishman 2000)

18.4.5 Direct Extension from Retroperitoneal Lymphoma

Contiguous extension from large retroperitoneal masses is the second most common pattern, present in 25–30% of cases (Fig. 18.15; Cohan et al. 1990). These patients usually have widespread disease with bulky tumors and many are immunocompromised. The CT appearance is that of large retroperitoneal masses invading or displacing the adjacent kidney (Fig. 18.16). Hydronephrosis caused by entrapment of the ureters is common; however, occlusion or thrombosis of major renal arteries and veins is rare despite extensive tumor encasement (Figs. 18.17, 18.18).

18.4.6 Perinephric Disease

Although perirenal spread from retroperitoneal lymphoma is not uncommon, isolated perinephric lymphoma is unusual, present in less than 10% of cases (Fig. 18.19; Cohan et al. 1990; Reznek et al.

a

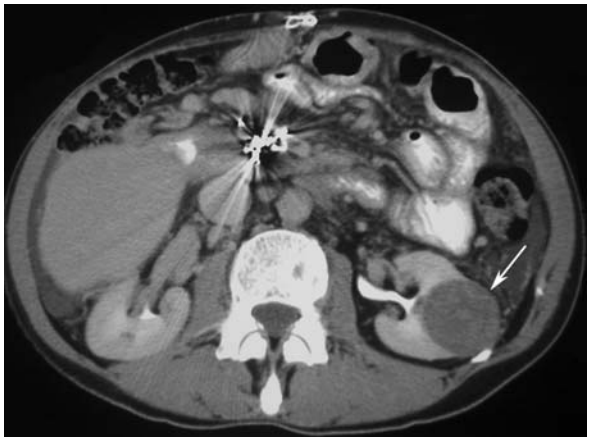

b

c

Fig. 18.14a-c. Papillary renal cell carcinoma mimicking lymphoma in a 57-year-old woman with history of liver transplant and a new renal mass. **a** Axial contrast-enhanced CT scan at the corticomedullary phase shows a hypovascular solitary mass (*arrow*) in the left kidney. This pattern is atypical for renal cell carcinoma. **b** Axial contrast-enhanced CT scan at the early excretory phase shows that the mass remains hypodense to the normal renal parenchyma in this phase (*arrow*). **c** Sagittal US image of the left kidney obtained at the time of biopsy shows a mildly echogenic mass (*calipers*). Note that lymphomas are generally hypoechoic. The pathological diagnosis based on the percutaneous biopsy was papillary renal cell carcinoma and the patient underwent a left nephrectomy. (With Permission from Urban and Fishman 2000)

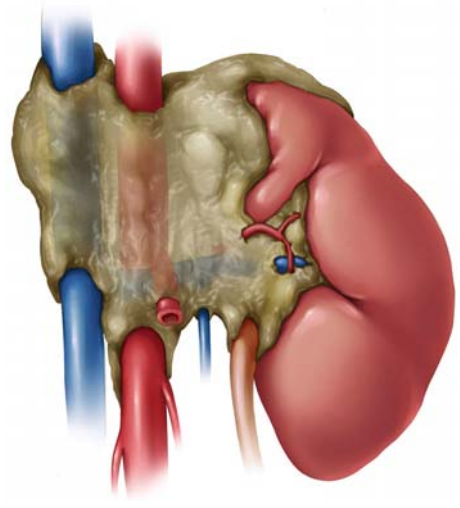

Fig. 18.15. The characteristic appearance of a bulky retroperitoneal mass invading the renal hilum and enveloping the renal vessels. (With Permission from Urban and Fishman 2000)

Fig. 18.16. Large B-cell non-Hodgkin's lymphoma in a 36-year-old HIV-positive woman. Axial contrast-enhanced CT scan of the abdomen shows a large heterogeneous left retroperitoneal mass extending into and infiltrating the left kidney (*arrows*). Note that the mass is encasing the left renal artery and vein.

1990). The CT images acquired after administration of intravenous contrast are invaluable to demonstrate a ring of homogeneous perinephric soft tissue compressing the normal parenchyma without causing significant impairment in renal function (Fig. 18.20). In less dramatic cases, findings include thickening of Gerota's fascia, or plaques and nodules in the perirenal space (Fig. 18.21; Sheeran

a

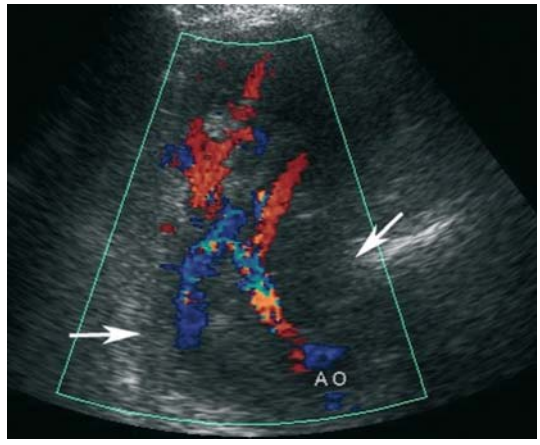

b

c

Fig. 18.17a-c. Burkitt lymphoma affecting the retroperitoneal nodes, adrenal glands, and both kidneys in a 46-year-old man. **a** Sagittal ultrasound image of the left kidney shows a large hypoechoic mass (*arrows*) displacing and infiltrating the left kidney. Note the mild left hydronephrosis. **b** Transverse color Doppler ultrasound image shows encasement of the left renal artery and vein by the mass (*arrows*). **c** Sagittal ultrasound image of the right kidney shows a hypoechoic renal mass (*arrow*). The right adrenal was also enlarged (not shown). (With Permission from Urban and 2000)

Fig. 18.18. Large B-cell lymphoma in a 52-year-old man with history of chronic lymphocytic leukemia. Axial contrast-enhanced CT scan shows tumor extension from the retroperitoneum into the right renal sinus fat and the perinephric space (*arrows*). Note delayed enhancement of the right kidney.

Fig. 18.19. The characteristic appearance of isolated perirenal lymphoma, which surrounds but does not destroy the underlying kidney. (With Permission from Urban and Fishman 2000)

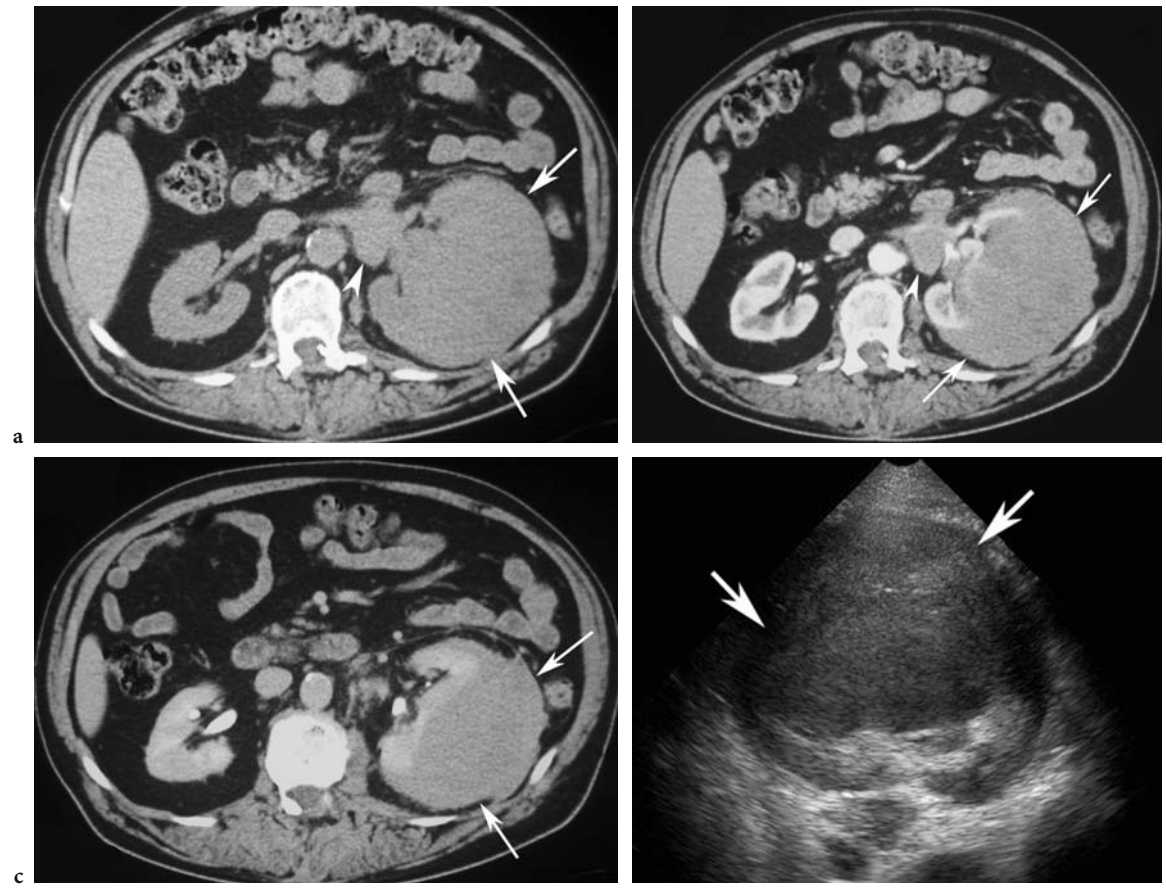

Fig. 18.20a-d. Incidental finding of left renal mass in a 66-year-old man. **a** Axial unenhanced CT scan shows marked enlargement of the left kidney (*arrows*). A left para-aortic lymph node is also present (*arrowhead*). **b** Axial contrast-enhanced CT scan in the corticomedullary phase shows a large hypovascular mass which is primarily in the perinephric space (*arrows*). The mass appears to invade the left renal parenchyma. Note that there is no significant delay in enhancement of the left renal parenchyma compared with the right kidney. **c** Axial contrast-enhanced CT scan in the excretory phase shows compression and invasion of the renal parenchyma by the mass (*arrows*). **d** Sagittal ultrasound image of the left kidney at the time of the biopsy shows a hypoechoic mass surrounding and partially invading the left kidney (*arrows*). Percutaneous biopsy yielded B-cell non-Hodgkin lymphoma. (With Permission from Urban and Fishman 2000)

and Sussman 1998). On US, hypoechoic tissue of variable thickness surrounds the kidney (Fig. 18.20; Cadman et al. 1988). Differential diagnoses to consider include sarcoma arising from the renal capsule and metastases to the perinephric space as well as benign conditions such as perinephric hematoma, retroperitoneal fibrosis, amyloidosis, and extramedullary hematopoiesis (Bechtold et al. 1996; Sheeran and Sussman 1998).

18.4.7 Nephromegaly

Nephromegaly without distortion of the normal reniform shape of the kidneys results from diffuse infiltration of the renal interstitium by malignant lymphocytes (Figs. 18.22, 18.23). This appearance is more common in Burkitt lymphoma, either the disseminated form or limited to the kidneys (primary renal lymphoma; Stallone et al. 2000). Acute renal failure caused by destruction of the normal renal architecture may bring the patient to seek medical attention. In such cases, both kidneys are usually affected.

Although the diagnosis can be suspected in the presence of global renal enlargement, administration of intravenous contrast is critical to demonstrate heterogeneous enhancement of the kidneys and loss of the normal differential enhancement between the cortex and the medulla in the corticomedullary phase. Alternatively, the renal parenchyma is replaced by poorly

a

b

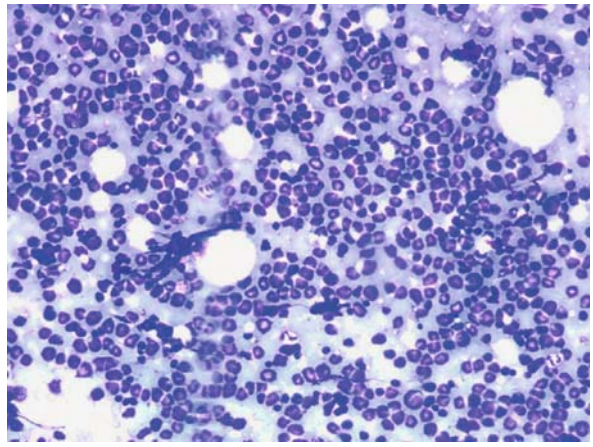

c

Fig. 18.21a-c. Routine follow-up CT in a 62-year-old man with a history of follicular non-Hodgkin lymphoma. **a** Axial contrast-enhanced CT scan in the portal venous phase shows a mildly enhancing mass in the right anterior pararenal space (*arrow*). This was a new finding for this patient. **b** Axial contrast-enhanced CT scan in the portal venous phase shows stranding in the mesenteric fat (*arrows*), suggestive of a "misty mesentery." This finding was also new. An ultrasound-guided biopsy of the perirenal mass yielded aggressive B-cell non-Hodgkin lymphoma. **c** Analysis of the fine-needle-aspiration sample shows malignant lymphocytes (Diff-Quik stain on site). (With Permission from Urban and Fishman 2000)

Fig. 18.22. The characteristic appearance of infiltrative lymphoma within the interstitium of the renal parenchyma. (With Permission from Urban and Fishman 2000)

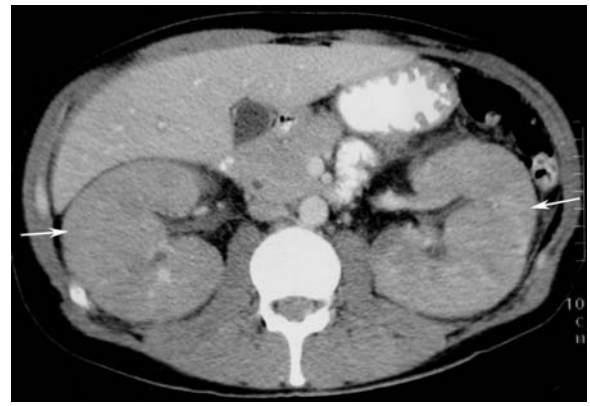

Fig. 18.23. Primary renal non-Hodgkin lymphoma involving both kidneys in a 41-year-old HIV-positive man who presented with renal failure. Axial contrast-enhanced CT scan of the kidneys in the nephrographic phase shows bilateral renal enlargement (*arrows*). There is heterogeneously decreased enhancement of the renal parenchyma. The diagnosis was established by renal biopsy. (With Permission from Urban and Fishman 2000)

defined hypodense lesions. The collecting system is often encased, stretched, or attenuated rather than displaced. Occasionally, lymphoma infiltrates and destroys the renal parenchyma extensively and presents as a large non-functioning kidney (Ambos et al. 1977; Hartman et al. 1988).

The US manifestations of infiltrative renal lymphoma are often subtle: they include globular enlargement of the kidneys with heterogeneous echotexture of the parenchyma and loss of the normal echogenic renal sinus (Hartman et al. 1988).

In some cases, the infiltrative process is unilateral or asymmetric. Diffuse infiltration of the kidney can also be caused by transitional cell carcinoma, collecting duct or medullary carcinoma of the kidneys, or severe pyelonephritis (Fig. 18.24).

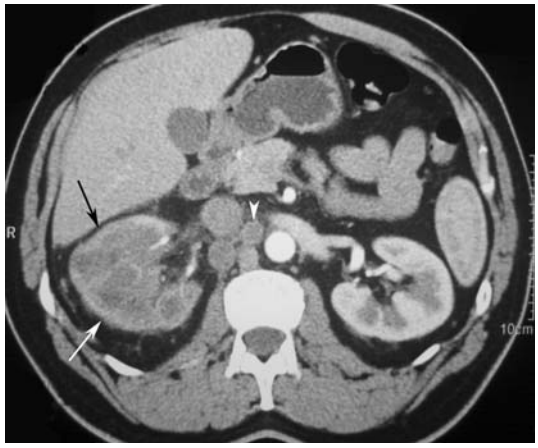

Fig. 18.24. Transitional cell carcinoma infiltrating the right kidney in a 44-year-old man with right flank pain. Contrast-enhanced CT in the corticomedullary phase shows a mass infiltrating the right kidney (*arrows*). Note that there is delayed enhancement in the right kidney and paracaval adenopathy (*arrowhead*). The diagnosis was established by percutaneous biopsy. (With Permission from Urban and Fishman 2000)

18.4.8 Renal Sinus Involvement

Lymphoma can affect the renal sinus, although this is uncommon. On CT, the normal renal sinus is replaced by a homogeneous soft tissue mass (Chang et al. 2002). The degree of enhancement within the mass is less than the normal parenchyma. Vascular encasement is common but, because of the pliable nature of the tumor, resulting hydronephrosis is often mild (Fig. 18.25). Transitional cell carcinoma is usually associated with a greater degree of obstruction to the collecting system. Castleman disease occurs occasionally in the renal hilum but cannot be differentiated without histological sampling (Nishie et al. 2003).

On US, this type of lymphoma appears as a hypoechoic mass infiltrating the renal sinus. This should be differentiated from heterogeneous sinus fat which is usually bilateral (Figs. 18.25, 18.26). If the mass is markedly hypoechoic, it can mimic hydronephrosis.

18.5 Role of Image-Guided Renal Biopsy in the Diagnosis of Renal Lymphoma

Image-guided percutaneous biopsy is a minimally invasive method to diagnose a variety of renal masses (Caoili et al. 2002). It is particularly helpful in avoiding unnecessary nephrectomy if the diagnosis of renal lymphoma is suspected on imaging (Stallone et al. 2000). Core biopsy as well as flow cytometric studies are useful to confirm the diagnosis and classify the lymphoma prior to therapy (Truong et al. 2001).

At our institution, US is the preferred guidance modality for percutaneous biopsy. Its real-time capability allows the needle to be guided into suspicious lesions under direct visualization, allowing for quick adjustment if necessary (Fig. 18.7). This results in faster procedure time compared with CT, as well as more accurate diagnosis even when the target is small or deep (Memel et al. 1996; Middleton et al. 1997). Lack of ionizing radiation, easy availability, and reduced cost are added benefits of US.

18.6 Conclusion

The urinary tract is a common site for extranodal spread of lymphoma, particularly non-Hodgkin lymphoma. Contrast-enhanced CT remains the preferred imaging modality for the detection of renal lymphoma. Magnetic resonance imaging is useful in special circumstances, particularly when the patient cannot tolerate intravenous contrast. Ultrasound has only a limited role except as a guidance modality for percutaneous biopsy.

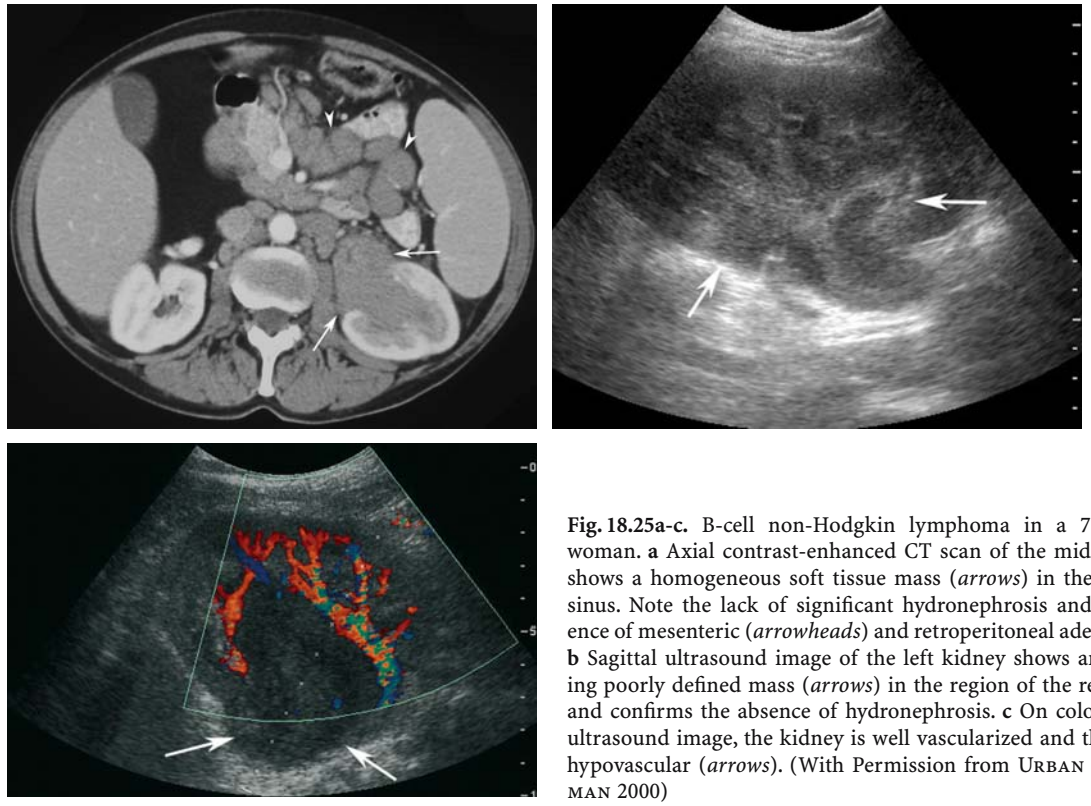

Fig. 18.25a-c. B-cell non-Hodgkin lymphoma in a 70-year-old woman. **a** Axial contrast-enhanced CT scan of the mid-abdomen shows a homogeneous soft tissue mass (*arrows*) in the left renal sinus. Note the lack of significant hydronephrosis and the presence of mesenteric (*arrowheads*) and retroperitoneal adenopathies. **b** Sagittal ultrasound image of the left kidney shows an infiltrating poorly defined mass (*arrows*) in the region of the renal pelvis and confirms the absence of hydronephrosis. **c** On color Doppler ultrasound image, the kidney is well vascularized and the mass is hypovascular (*arrows*). (With Permission from Urban and Fishman 2000)

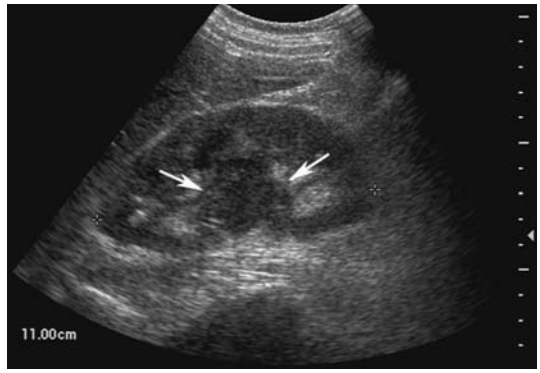

Fig. 18.26. Recurrent Hodgkin disease in a 29-year-old man presenting as a right renal hilar mass. Sagittal ultrasound image of the right kidney shows an ill-defined hypoechoic mass (*arrows*) infiltrating the renal sinus fat. The diagnosis was confirmed by percutaneous fine-needle aspiration and core biopsy performed under ultrasound guidance. (With Permission from Urban and Fishman 2000)

References

Ambos MA, Bosniak MA, Madayag MA, Lefleur RS (1977) Infiltrating neoplasms of the kidney. Am J Roentgenol 129:859–864

Bechtold RE, Dyer RB, Zagoria RJ, Chen MY (1996) The perirenal space: relationship of pathologic processes to normal retroperitoneal anatomy. Radiographics 16:841–854

Cadman PJ, Lindsell DR, Golding SJ (1988) An unusual appearance of renal lymphoma. Clin Radiol 39:452–453

Caoili EM, Bude RO, Higgins EJ, Hoff DL, Nghiem HV (2002) Evaluation of sonographically guided percutaneous core biopsy of renal masses. Am J Roentgenol 179:373–378

Chang SS, Nayak R, Cookson MS (2002) Lymphoma presenting as a solitary renal hilar mass. Urology 59:134–135

Chepuri NB, Strouse PJ, Yanik GA (2003) CT of renal lymphoma in children. Am J Roentgenol 180:429–431

Cohan RH, Dunnick NR, Leder RA, Baker ME (1990) Computed tomography of renal lymphoma. J Comput Assist Tomogr 14:933–938

Eisenberg PJ, Papanicolaou N, Lee MJ, Yoder IC (1994) Diagnostic imaging in the evaluation of renal lymphoma. Leuk Lymphoma 16:37–50

Guermazi A, Brice P, de Kerviler E, Ferme C, Hennequin C, Meignin V, Frija J (2001) Extranodal Hodgkin disease: spectrum of disease. Radiographics 21:161–179

Harisinghani MG, Maher MM, Gervais DA, McGovern F, Hahn P, Jhaveri K, Varghese J, Mueller PR (2003) Incidence of malignancy in complex cystic renal masses (Bosniak category III): Should imaging-guided biopsy precede surgery? Am J Roentgenol 180:755–758

Hartman DS, David CJ Jr, Goldman SM, Friedman AC, Fritzsche P (1982) Renal lymphoma: radiologic–pathologic correlation of 21 cases. Radiology 144:759–766

Hartman DS, Davidson AJ, Davis CJ Jr, Goldman SM (1988) Infiltrative renal lesions: CT–sonographic–pathologic correlation. Am J Roentgenol 150:1061–1064

Heiken JP, Gold RP, Schnur MJ, King DL, Bashist B, Glazer HS (1983) Computed tomography of renal lymphoma with ultrasound correlation. J Comput Assist Tomogr 7:245–250

Malbrain ML, Lambrecht GL, Daelemans R, Lins RL, Hermans P, Zachee P (1994) Acute renal failure due to bilateral lymphomatous infiltrates. Primary extranodal non-Hodgkin's lymphoma (p-EN-NHL) of the kidneys: does it really exist? Clin Nephrol 42:163–169

Memel DS, Dodd GD III, Esola CC (1996) Efficacy of sonography as a guidance technique for biopsy of abdominal, pelvic, and retroperitoneal lymph nodes. Am J Roentgenol 167:957–962

Metser U, Goor O, Lerman H, Naparstek E, Even-Sapir E (2004) PET-CT of extranodal lymphoma. Am J Roentgenol 182:1579–1586

Middleton WD, Hiskes SK, Teefey SA, Boucher LD (1997) Small (1.5 cm or less) liver metastases: US-guided biopsy. Radiology 205:729–732

Mills NE, Goldenberg AS, Liu D, Feiner HD, Gallo G, Gray C, Lustbader I (1992) B-cell lymphoma presenting as infiltrative renal disease. Am J Kidney Dis 19:181–184

Moog F, Bangerter M, Diederichs CG, Guhlmann A, Merkle E, Frickhofen N, Reske SN (1998) Extranodal malignant lymphoma: detection with FDG PET versus CT. Radiology 206:475–481

Nishie A, Yoshimitsu K, Irie H, Aibe H, Tajima T, Shinozaki K, Nakayama T, Kakihara D, Naito S, Ono M, Muranaka T, Honda H (2003) Radiologic features of Castleman's disease occupying the renal sinus. Am J Roentgenol 181:1037–1040

Pickhardt PJ, Lonergan GJ, Davis CJ Jr, Kashitani N, Wagner BJ (2000) From the archives of the AFIP. Infiltrative renal lesions: radiologic–pathologic correlation. Armed Forces Institute of Pathology. Radiographics 20:215–243

Reznek RH, Mootoosamy I, Webb JA, Richards MA (1990) CT in renal and perirenal lymphoma: a further look. Clin Radiol 42:233–238

Richards MA, Mootoosamy I, Reznek RH, Webb JA, Lister TA (1990) Renal involvement in patients with non-Hodgkin's lymphoma: clinical and pathological features in 23 cases. Hematol Oncol 8:105–110

Richmond J, Sherman RS, Diamond HD, Craver LF (1962) Renal lesions associated with malignant lymphomas. Am J Med 32:184–207

Semelka RC, Kelekis NL, Burdeny DA, Mitchell DG, Brown JJ, Siegelman ES (1996) Renal lymphoma: demonstration by MR imaging. Am J Roentgenol 166:823–827

Sheeran SR, Sussman SK (1998) Renal lymphoma: spectrum of CT findings and potential mimics. Am J Roentgenol 171:1067–1072

Stallone G, Infante B, Manno C, Campobasso N, Pannarale G, Schena FP (2000) Primary renal lymphoma does exist: case report and review of the literature. J Nephrol 13:367–372

Szolar DH, Kammerhuber F, Altziebler S, Tillich M, Breinl E, Fotter R, Schreyer HH (1997) Multiphasic helical CT of the kidney: increased conspicuity for detection and characterization of small (<3 cm) renal masses. Radiology 202:211–217

Truong LD, Caraway N, Ngo T, Laucirica R, Katz R, Ramzy I (2001) Renal lymphoma. The diagnostic and therapeutic roles of fine-needle aspiration. Am J Clin Pathol 115:18–31

Urban BA, Fishman EK (2000) Renal lymphoma: CT patterns with emphasis on helical CT. Radiographics 20:197–212

Weinberger E, Rosenbaum DM, Pendergrass TW (1990) Renal involvement in children with lymphoma: comparison of CT with sonography. Am J Roentgenol 155:347–349

Yasunaga Y, Hoshida Y, Hashimoto M, Miki T, Okuyama A, Aozasa K (1997) Malignant lymphoma of the kidney. J Surg Oncol 64:207–211